



**HAL**  
open science

# Assessment of damage induced in masonry structures by soil subsidence using physical modelling

Luyen Nghiem, Fabrice Emeriault, Marwan Al Heib

## ► To cite this version:

Luyen Nghiem, Fabrice Emeriault, Marwan Al Heib. Assessment of damage induced in masonry structures by soil subsidence using physical modelling. 9. International Masonry Conference, Jul 2014, Guimaraes, Portugal. ineris-01862441

**HAL Id: ineris-01862441**

**<https://ineris.hal.science/ineris-01862441>**

Submitted on 27 Aug 2018

**HAL** is a multi-disciplinary open access archive for the deposit and dissemination of scientific research documents, whether they are published or not. The documents may come from teaching and research institutions in France or abroad, or from public or private research centers.

L'archive ouverte pluridisciplinaire **HAL**, est destinée au dépôt et à la diffusion de documents scientifiques de niveau recherche, publiés ou non, émanant des établissements d'enseignement et de recherche français ou étrangers, des laboratoires publics ou privés.

# Assessment of damage induced in masonry structures by soil subsidence using physical modelling

NGHIEM, HUU-LUYEN<sup>1</sup>; EMERIAULT, FABRICE<sup>2</sup>; AL HEIB, MARWAN<sup>3</sup>

**ABSTRACT:** Masonry structures can be deformed by deferred settlement and damaged. This paper presents the experimental results obtained on masonry due to subsidence effects taking soil-structure interaction into account. A new approach is proposed here for the assessment of damage levels based on physical modelling combined with digital image correlation (DIC) technique. The physical model has dimensions of 3\*2\*1 m with a 1/40 scale factor on geometry, functions under the normal gravity and uses sand as the analogue soil and an assemblage of small wooden pieces for the analogue masonry. A ground settlement profile is applied using a mechanical-electrical jack. In particular, a new indicator is developed for a damage-based performance assessment with particular attention to masonry structures. This indicator enables the location of the damage to be identified and quantified, and can be implemented in numerical models. Guidelines are suggested for efficient damage estimation.

*Keywords: masonry structure, crack identification, damage assessment, physical modelling, small-scale model, digital correlation image.*

## NOTATIONS

$R$  rotation tensor;  
 $c$  translation vector;  
 $e$  distance from the centre of the structure to centre of the curvature;  
 $B$  length of the structure;  
 $H$  height of the structure;  
 $W_c$  critical width of mine area;  
 $D$  depth of mine area;  
 $O$  layer opening;  
 $e/B$  relative eccentricity of the structure compared with the centre of curvature;  
 $\Delta/B$  relative deflexion;  
 $\varepsilon$  deformation;  
 $\Delta u$  crack width;  
 $L^*_{Di}$  relative length of cracks associated with the damage class  $D_i$ ;

---

<sup>1</sup> Ph.D student, INERIS, Parc technologique Alata, 60550 Verneuil-En-Halatte, France, Huu-Luyen.Nghiem@ineris.fr

<sup>2</sup> Professor, Grenoble-INP, UJF-Grenoble 1, CNRS UMR 5521, 3SR Lab, Grenoble F-38041, France.Fabrice.Emeriault@grenoble-inp.fr

<sup>3</sup> HDR, INERIS, Parc technologique Alata, 60550 Verneuil-En-Halatte, France, Marwan.Alheib@ineris.fr

# 1 INTRODUCTION

Land subsidence results in some of the worst possible conditions for civil engineering projects and construction. The collapse of soil cover over cavities can damage vulnerable existing structures such as buildings and infrastructures. Risk management is critical for underground and new building construction projects. The building is mostly considered to be an elastic beam. Some parameters for damage assessment, such as the angular distortion [1], the deflexion ratio [2], and the relative stiffness associated to angular distortion and deflexion ratio [3, 4] are available in the literature. These parameters associate the damage levels with the tensile limit strain [1]. They can be useful for assessing the damage level in a preliminary analysis. Nevertheless, they are highly idealized and often over- or under-estimate the potential level of structural damage.

Approaches using physical models [5, 6] have recently been developed in order to improve the knowledge of the complex behaviour in the occurrence of subsidence. Nevertheless, these investigations are limited to the observation of crack propagation. Consequently, analysis has focused only on crack location and has failed to tackle the problem of damage quantification.

In this study, we introduce a new performance indicator for assessing damage to masonry structures, i.e., the total length of cracks in addition of the maximum width of the cracks. Here, we discuss a new point of view for crack identification, which is the purpose of the physical modelling combined with an experimental criterion for crack opening. The proposed physical model is a small-scale mock-up of a typical individual house in a subsidence area (mostly masonry structures). The displacement fields are monitored using a Digital Image Correlation (DIC) technique, and the reconstruction of blocks is required in order to identify opening between blocks (i.e., cracks). In this step, the displacements of each block are broken down into two parts: rotation and translation. The criterion for a “crack” refers to the crack width at the interface between blocks according to the damage categories defined by Burland [7]. In addition, this paper also analyses the influence of structural positions with respect to the settlement trough on the damage levels. Three main critical positions are considered for the structure: sagging zone, hogging zone, and mixed zone of a subsidence trough induced by underground excavation. At the same time, a mechanical interpretation is given using both the conventional and the new indicators.

## 2 PHYSICAL MODELLING FOR MASONRY STRUCTURE

### 2.1. State of the art

Physical modelling is the origin of the dimensional analysis and is based on Buckingham’s theorem [8]. Theoretically, the concept of the physical model must respect laws of similitude (see [9]). Nevertheless, similarity is not always observed between the prototype and model. The difficulty is often related to the choice of materials and equipment available under laboratory conditions. Depending on the physical quantity, we can limit to the physical modelling of phenomena using the restrained similitude of geometry, deformation, material, etc. Likewise, the physical model proposed in this paper chiefly respects geometric similarity (distance, area, volume) under normal gravity (1g) in order to study the similitude of the displacements.

The subsidence profile in case of greenfield (absence of building on the surface) is generally characterized by the amplitude of subsidence and the influence angle. With the presence of the structure at the ground surface, some additional parameters are defined to describe the effect of the soil-structure interaction, such as deformation, slope, deflexion and curvature of the structure (see [10, 11]). In order to reproduce the phenomena and assess the vulnerability of masonry structures (typically individual houses), a large small-scale physical model was designed (Figure 1b and c). This model is equivalent to the prototype of an ordinary house found in hazard zones (for example, former coal and iron mining zones in northeastern France), its typical dimensions being  $10 \times 10 \text{ m}^2$  and the

cavity depth being 12 m. The use of 40<sup>th</sup> scale factor provides dimensions 0.25x0.25 m<sup>2</sup> for the model. The behaviour of the masonry structure depends on the physical model and initial conditions. The initial condition in Figure 1b presents two particular interfaces: block-silicon  $\Gamma_1$  and silicon-sand  $\Gamma_2$ , the silicone corresponding to the foundation in contact with the soil (sand layer). The first interface  $\Gamma_1$  has perfect bounding, which insures the continuity of displacements. It is also helpful for easy implementation of the model in the platform. The second interface  $\Gamma_2$  is a simple frictional contact of the silicon foundation with sand maintained by the normal force applied by the weight of the structure.

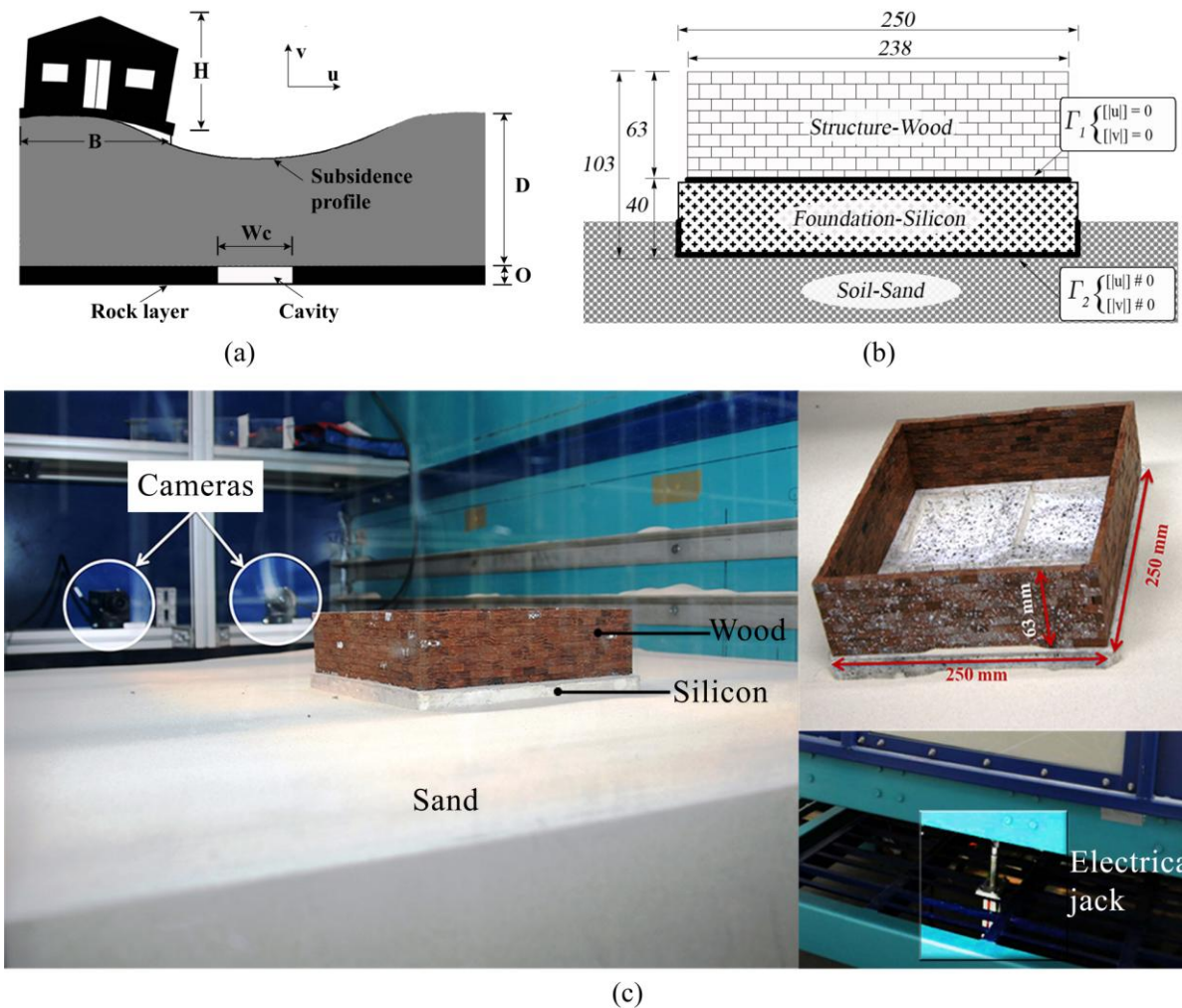


**Figure 1.** Description of the problem. a) Building on surface. b) 2D cross-section – distances in mm. c) INERIS physical model (1/40 scale factor)

The choice of materials is extensively discussed in recent works [10]. The analogue soil that represents ground above the cavity is the Fontainebleau sand (essentially silica with  $\text{SiO}_2 > 98\%$ ) and an initial relative density of 44% (medium dense conditions). For the analogue structure, different models have been suggested and tested such as polycarbonate slab, silicon slab, sugar blocks, and wooden blocks. The wooden blocks solution is the most realistic (see [10]) and has been chosen in this investigation.

## 2.2. Digital Image Correlation technique

Digital Image Correlation (DIC) is a contactless method of displacement measurement using video cameras to record images of the surface of an object. This technique is used nowadays in a wide

range of disciplines, particularly in the mechanical testing of materials and structures. In this project, the commercial software VIC-3D from Limesh GmbH was chosen, which provides full-field, 3-dimensional measurements of shape, displacement and strain. Four high-resolution cameras were used with a maximum frequency of 8 images/second. The two first cameras are dedicated to recording images of the masonry façade, and the other two are set up with the purpose of investigating the sand movements. A good calibration enables accurate measurements to be obtained with an error of 1/100 of a pixel. The recording of images requires a huge volume of data storage. A single test produces nearly 8 GB of raw data for each minute when the maximum capture frequency is used.

### 2.3. Test procedure

The test procedure can be summarized in three main steps: 1) The tank is first filled with a homogeneous layer of Fontainebleau sand (a specific procedure has been defined in order to obtain a uniform density over the 0.30 thick layer). 2) The subsidence is reproduced using the mechanical-electrical jack with a sufficiently low speed (0.15 mm/s) to create the vertical displacement of a 250x250 mm plate at the bottom of the tank. The displacements of the ground surface and of the structure are captured by four rapid high-resolution cameras (using the VIC-Snap software). 3) The images are analysed using the VIC-3D software in order to determine the displacement fields in the 3 directions and calculate the corresponding strain fields.

## 3 DAMAGE INDICATOR

### 3.1. Reconstruction of masonry based on Digital Image Correlation

The displacement fields obtained using “standard” DIC are generally described in the context of a continuous material. However, the masonry is usually considered as a discrete system due to units and mortar. Furthermore, damage is generally localized at the joints between blocks (crack opening). In order to conform to this description, we have to break down the displacement fields at the level of individual blocks into two parts: rotation and translation of blocks. As a first step, we need to identify the interface between blocks. The idea is to create an equivalent system with blocks having the same coordinates in the DIC system. As the size and the number of blocks are known, the equivalent masonry wall can be constructed by the translation of a block in horizontal and vertical directions (thus creating layers). A common point for the equivalent and DIC systems is required with the purpose of seeking the same blocks. As a result, the interfaces between blocks and their normal vectors are well known.

In order to identify the displacement of the blocks, the main idea is the use of polar decomposition, which allows the displacement field to be expressed purely using rotation and deformation terms. To do this, we consider each block as an arbitrary body  $\Omega_0$  at the initial time  $t_0=0$  and the current configuration  $\Omega_t$  at the time  $t$ . The displacement of a material point is expressed by the application  $\varphi: (\Omega_0 \times P) \rightarrow \Omega_t$ , which is the transformation of the point  $X \in \Omega_0$  at time  $t \in [0, T]$  to the point  $x = \varphi(X, t) \in \Omega_t$  at time  $t$ . The displacement of point  $X$  at time  $t$  is denoted by  $u(X, t) = \varphi(X, t) - X$ . Using a Lagrangian description, the transformation gradient has the form of a fourth-order tensor defined by  $F = \nabla \varphi$ . Then, the tensor  $F$  in the polar decomposition becomes  $F = R \cdot U$ , where  $R$  denotes the pure rotation tensor and  $U$  is the pure deformation tensor. Because the blocks are considered as rigid bodies, the pure rotation term of the transformation tensor reads as follows:

$$R = F \tag{1}$$

$$c = x - R \cdot X - G_0 \quad (2)$$

$G_0$  is the centre of rotation, which is a delicate point. Theoretically, this can be identified when two rotations of block at two different times are known. This can be overcome by considering the slow load of the test and the centres of rotation are identical at time  $t$  and  $t+1$ . However, the obtained data of DIC have usually some noise, so these hypotheses are no longer accurate. Consequently, we consider  $G_0$  as the gravity centre of the block, and a cost function is needed in order to ascertain that the difference of the model and experimental displacements is less than an error tolerance (5%). The last one is considered as a stop criterion of the cost function.

### 3.2. Total length of cracks

The use of physical modelling allows integration of an experimental criterion for cracks that respects the law of the similitude of displacements. Here, we use the damage classes proposed by Burland in Table 1. The first three classes  $D_0$ ,  $D_1$ , and  $D_2$  correspond to aesthetic damage to a masonry structure. Classes  $D_3$  and  $D_4$  involve functional damage and affect serviceability. Class  $D_5$  is structural damage affecting the integrity and the stability of the masonry structure. The damage class is related to the intensity of the deflection ratio or/and horizontal strain of the structure.

**Table 1.** Damage classification scale of a masonry structure [7]

| Id    | Damage class | Crack width (mm)                               |
|-------|--------------|--|
| $D_0$ | Negligible   | 0-0.1 mm                                       |
| $D_1$ | Very slight  | 0.1-1 mm                                       |
| $D_2$ | Slight       | 1-5 mm   |
| $D_3$ | Moderate     | 5-15 mm or a number of cracks > 3 mm           |
| $D_4$ | Severe       | 15-25 mm, but also depends on number of cracks |
| $D_5$ | Very severe  | > 25 mm, but depends on numbers of cracks      |

The crack propagation in the masonry wall has a particular property here: it appears only at the level of the joints, which is to say that cracks appear when the blocks move apart. Thus, crack identification is equivalent to the determination of opening between blocks. Because the interfaces and their normal vectors are known, the opening between blocks is determined as follows:

$$\Delta u = \mathbf{u}_1 \cdot \mathbf{n}_1 + \mathbf{u}_2 \cdot \mathbf{n}_2 \quad (3)$$

$\mathbf{u}_1$ ,  $\mathbf{u}_2$  are displacement vectors on the considered interface and  $\mathbf{n}_1$ ,  $\mathbf{n}_2$  are their respective normal vectors. In Equation (3), a negative value for  $\Delta u$  indicates that the blocks are moving apart and that cracks are appearing. Nevertheless, the actual model of the structure cannot be made with perfect contact conditions between all of the blocks. This leads to an initial situation where joints can be opened from the onset. In addition, the evolution of the subsidence trough can lead to a partial closure of the opened joint. Therefore, we can eliminate this default by taking into account the positive value of  $\Delta u$  in Equation (3).

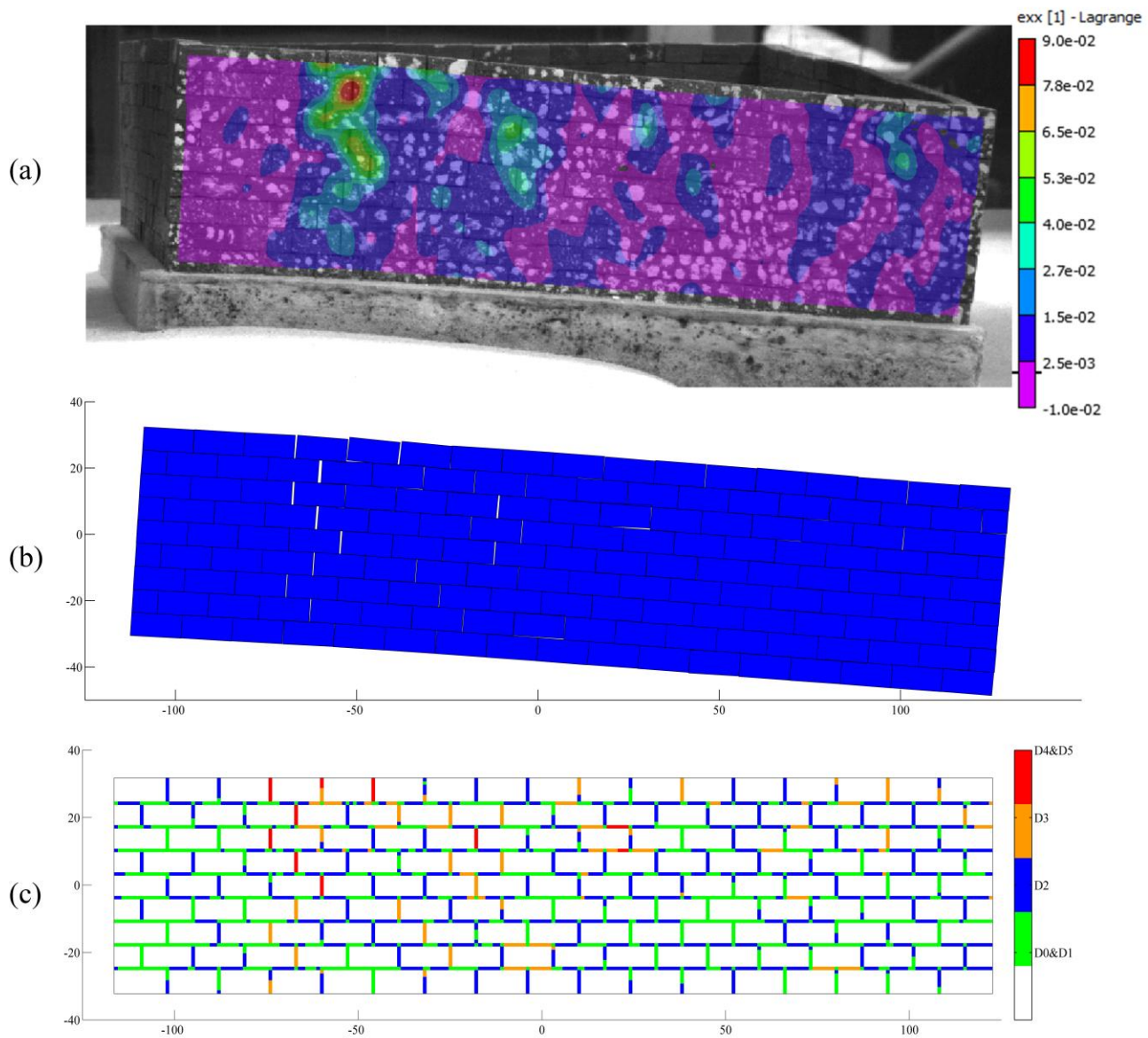


**Figure 2.** Example of the numerical reconstruction of an observed masonry wall. a) Horizontal Lagrangian strain provided by VIC-3D software. b) Location of cracks. c) Identification of damage classes (from slight to severe).

The main indicator for the damage evaluation is the relative total length of cracks, which is the total length of cracks compared to the total length of the joints. A value is determined for each damage class as follows:

$$L_{Di}^* = \frac{\sum l_{Di}}{L_0} \quad (4)$$

where  $\sum l_{Di}$  is the length of joints in class  $D_i$  and  $L_0$  is the total length of the joints.

Figure 2 presents the results of the reconstruction step compared to the distribution of the horizontal Lagrangian strain provided by the VIC-3D software. The bias error of strain is at least  $1.5 \times 10^{-20}\%$  inside the rigid blocks (Figure 2a), which cannot be accepted in reality. The reconstruction of blocks allows this inconvenience to be overcome, with blocks having no strain inside and cracks

appearing only at the level of the joint (Figure 2b). Furthermore, this reconstruction step can locate the damage class for each joint as shown in Figure 2c. Consequently, the damage can be completely assessed using three important properties of cracks: width, length, and position. For example, Figures 2a and b reveal a relation between the position of the cracks in the wall and the soil-structure contact area, i.e. a concentration of numerous cracks in this contact area.

### 3.3. Measurement noise

Although DIC is a powerful technique for mechanical tests, the test results can be affected by numerous errors and uncertainties, such as the quality of the measurement devices, the working environment and the correlation algorithms. The first one is associated with the material, e.g. optical lens. The second is linked to the working environment such as the epipolar constraint, the process of calibration, lighting, etc. The third category concerns the choice of correlation parameters such as subset size, speckle pattern, and cost functions. In order to evaluate the measurement errors, we have adopted the strategy of taking the first series of deformed images to determine the crack width  $\Delta u$  of Equation (3). The values for  $\Delta u$  can be computed from the points of the interfaces. A regular mesh is currently used for the discretization of the interfaces.

Values obtained for  $\Delta u$  are represented by the “frequency” in Figure 3a, linked to the number of points, and the corresponding probability in Figure 3b. From the latter, it can be concluded that, for 95% of the points the measured, the crack width is smaller than 0.45 mm. According to the damage classes in Table 1, this is indicative of classes  $D_0$  (0 to 0.1 mm) and  $D_1$  (0.1 to 1 mm). Therefore, the total length of cracks is no longer accurate for the first two classes, so we group them into only one class, denoted as  $D_{0\&1}$ .

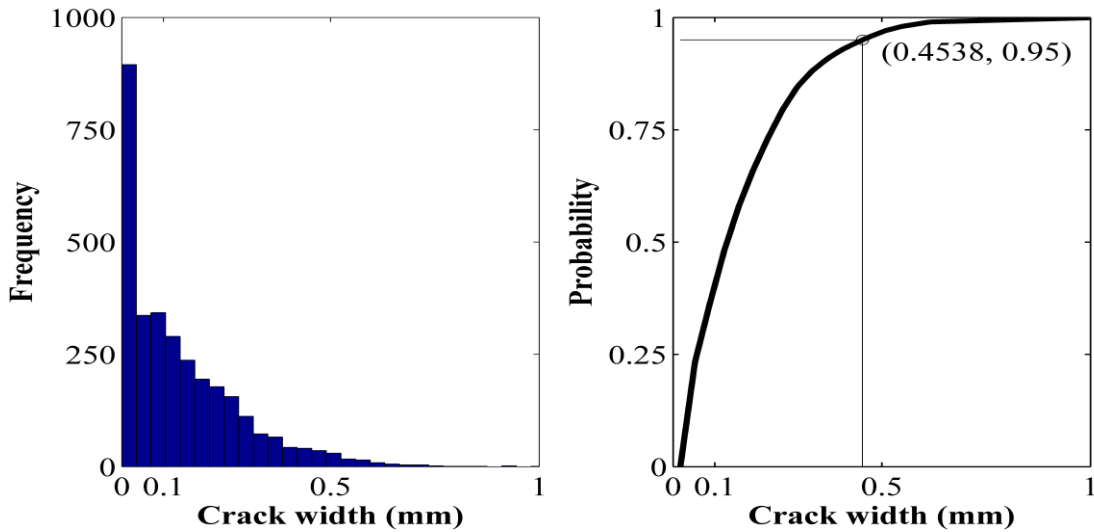


**Figure 3.** Measurement noise of the DIC technique. a) Distribution of crack width for the points of interface between blocks. b) Probability curve.

## 4 EXPERIMENTAL RESULTS

This section compares the results of the tests for three critical positions of the structure: position  $P_1$  in the sagging zone with the relative eccentricity  $\frac{e_x}{B}=0, \frac{e_y}{B}=0$ , position  $P_2$  in the hogging zone ( $\frac{e_x}{B}=0,5, \frac{e_y}{B}=0,5$ ), and position  $P_3$  in the mixed zone  $P_3$  ( $\frac{e_x}{B}=0,5, \frac{e_y}{B}=0$ ). The term “ $e$ ” is the distance from the centre of the subsidence trough to the centre of the structure, and “ $B$ ” is the length of the structure. Figure 4 shows the setup of the positions and the observed masonry façade. Only one wall is observed here due to a lack of equipment and given the working environment. In particular, the



structure with position  $P_3$  completely collapsed when the jack displacement reached 20 mm. In addition; Figure 4 also captured the final states of the structures in the different positions. Moreover, the soil displacements are not discussed in this investigation because correlation of images was lost. In fact, the structure hides a significant portion of the soil and DIC cannot analyze this section.

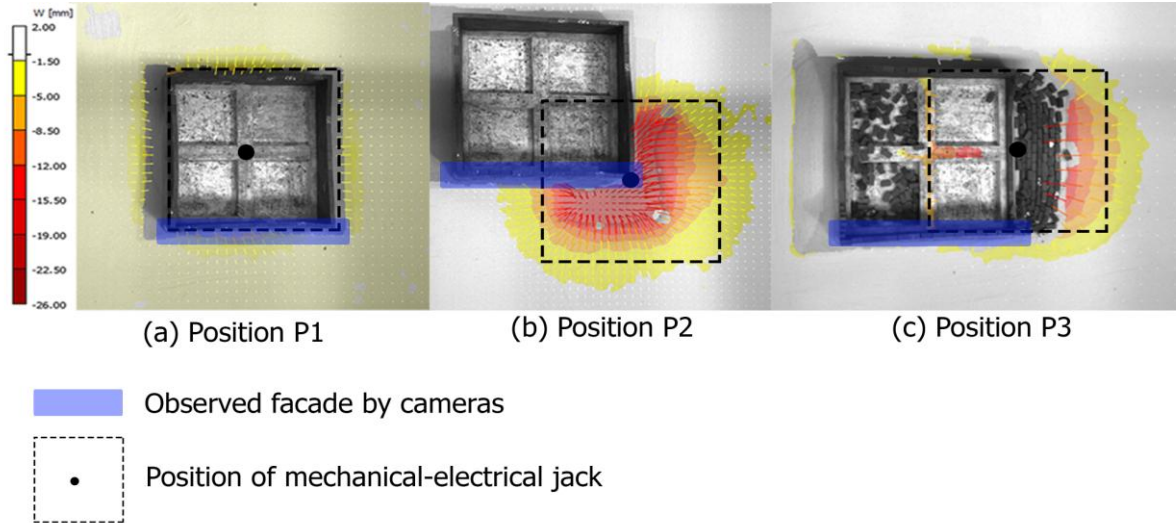


**Figure 4.** Three critical positions of the structure in a subsidence area: (a) sagging zone, (b) hogging zone, and (c) mixed zone (tension in the x direction and compression in the y direction).

The parameters used in the VIC-3D software (see [12]) are: subset=17 pixels and step=2, which provide more than  $3 \times 10^4$  points for each image. For the reconstruction step, the interfaces between blocks are identified using a regular grid of  $238 \times 63 \text{ mm}^2$ , with the size of the grid being  $h=1 \text{ mm}$ . As a result, there are a total of 3096 points for the interfaces.

#### 4.1. Conventional parameters

To identify the damage level in a masonry structure the following parameters are usually used: the average slope, the relative maximal deflexion, and the maximal deformation of the structure as shown in Figure 5. The average slope is the gradient of the vertical displacements which are calculated from the two extremities of the foundation. The relative maximal deflexion refers to the relative value of the maximal deflexion of the foundation divided by the length of the hogging/sagging zone (see [3]). And the maximal deformation is linked to the extension length of the structure.

Figure 5a shows that position  $P_1$  is more stable than positions  $P_2$  and  $P_3$ , with average slope values of less than 1%. In fact, the slope values are almost zero when the jack displacement is less than 20 mm, then increase slightly. The reason for this is the zero eccentricity of the structure, which leads to homogenous displacements of the soil. The disturbed movements of the soil cause an incrementing of the slope in the final state. Position  $P_2$  is characterized by a linear trend, while the evolution for position  $P_3$  is non-linear and always below the slope measured for  $P_2$ . This means that the structure in  $P_2$  has more damage than that in  $P_3$ , which can be explained by the absence of restraint in the y direction compared to  $P_3$ , which maintains a slow settlement of the structure in the x direction. According to the typical values for maximum building slope and settlement proposed for damage risk assessment by CIRIA PR30, 1996 (see [13]), damage is considered to be “negligible” when the maximum slope is between 0 and 0.2%, “slight” damage corresponds to values between 0.2 and 0.5%, moderate damage falls between 0.5 and 2%, and for high damage the slope is greater than 2%. In the final state,  $P_1$  presents a slope of 1.0%, which is close to the moderate damage class, whereas for the other two positions the slopes are over the high damage class: 7.3% for  $P_2$  and 4.5% for  $P_3$  (measured values when the jack displacement reaches 20 mm). The structures enter the high damage class, i.e., the slope is superior to 2%, when the jack displacement reaches 8 mm for  $P_2$  and 12 mm for  $P_3$ .

The deflexion ratios are shown in Figure 5b. The structures in  $P_2$  and  $P_3$  are in the convex state with positive values, while  $P_1$  is in the concave state with negative values. For  $P_1$ , the evolution is slightly linear, with a final value of  $-0.6\%$ ; in  $P_2$ , the increase is linear for the first time when the jack displacement is less than 10 mm, then remains constant during the rest of the test ( $0.5\%$  at the final state);  $P_3$ , in turn, exhibits a non-linear curve with a value of  $1.1\%$  when the jack displacement reaches 20 mm. In the final state, the structure in  $P_3$  has the largest deflection value, i.e., this position causes the most significant damage to the structure. Besides, according to the study of *Potts et al.* [3],  $P_1$  and  $P_2$  having similar values for deflexion and identical structural rigidity are classed into the same category of damage. This is very questionable in view of the deformation of the structure and the number of cracks in the wall. In fact, both quantities are larger for  $P_2$  than for  $P_1$  (see Figure 5c and 6). Similar results have been obtained in recent papers [14]: For the three positions in the final state (30 mm of jack displacement), the structures are in the severe & very severe damage class.

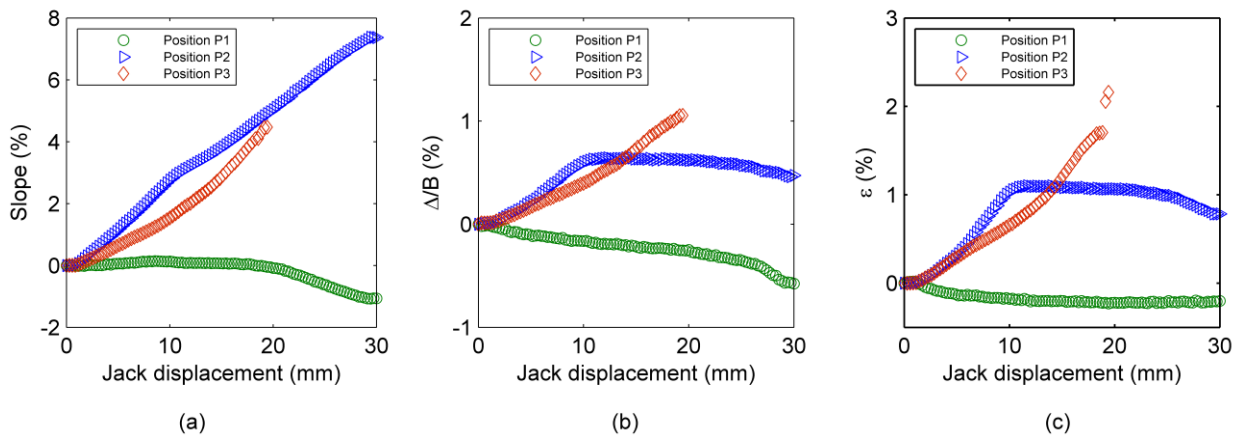


**Figure 5.** Conventional parameters for damage evaluation. a) Average slope. b) Relative maximal deflexion. c) Deformation of structure.

The third conventional parameter linked to the deformation of the structure is presented in Figure 5c. The three positions provide trends similar to that of the deflexion in Figure 5b. However, the final values are significantly different:  $-0.2\%$  for  $P_1$ ,  $0.8\%$  for  $P_2$ , and  $2.1\%$  for  $P_3$ . According to the damage classification in [1], the damage levels depend on the limiting tensile strain and break down into negligible damage (0 to  $0.05\%$ ), very slight damage ( $0.05$  to  $0.075\%$ ), slight damage ( $0.075$  to  $0.15\%$ ), moderate damage ( $0.15$  to  $0.3\%$ ), and severe damage ( $>0.3\%$ ). Compared to the values of the tests,  $P_1$  has moderate damage with a deformation of  $0.2\%$ , and  $P_2$  and  $P_3$  correspond to the severe damage class:  $0.8\%$  for  $P_2$  and  $2.1\%$  for  $P_3$ . Nevertheless,  $P_3$  provides the most significant deformation. Consequently,  $P_3$  is the most damaged, while  $P_1$  presents the least damage according to the deformation parameter.

Deflexion and deformation have an inferential relationship, i.e., an increase in deflexion leads to an increase in deformation. Therefore, damage can be assessed using a combination of the two above parameters, as in Burland's method [2]. According to this method, for a deflexion over  $0.35\%$ , the structure is considered to be severely damaged regardless of the deformation value. As a result, all positions in the final state of the tests are in the severe class because of their high deflexions:  $0.6\%$  for  $P_1$ ,  $0.5\%$  for  $P_2$ , and  $1.1\%$  for  $P_3$  (Figure 5b). Nevertheless, this approach seems to overestimate the real damage of the structure. In particular,  $P_1$  should be deemed to be moderately damaged with respect the slope, the deformation, and the number of cracks.

#### 4.2. "Indicator" of total length of cracks

The three above parameters pose some disadvantages for the assessment of structural damage due to subsidence. Due to the fact that the structure is idealised as an equivalent beam, the damage levels are usually under- or over-estimated. This can be overcome by using the indicator related to

the total length of cracks and their positions on the structure. Figure 6 illustrates the quantification of damages following the three positions of the structure. This assessment is based on the notion of relative length of cracks as defined in Equation (4).

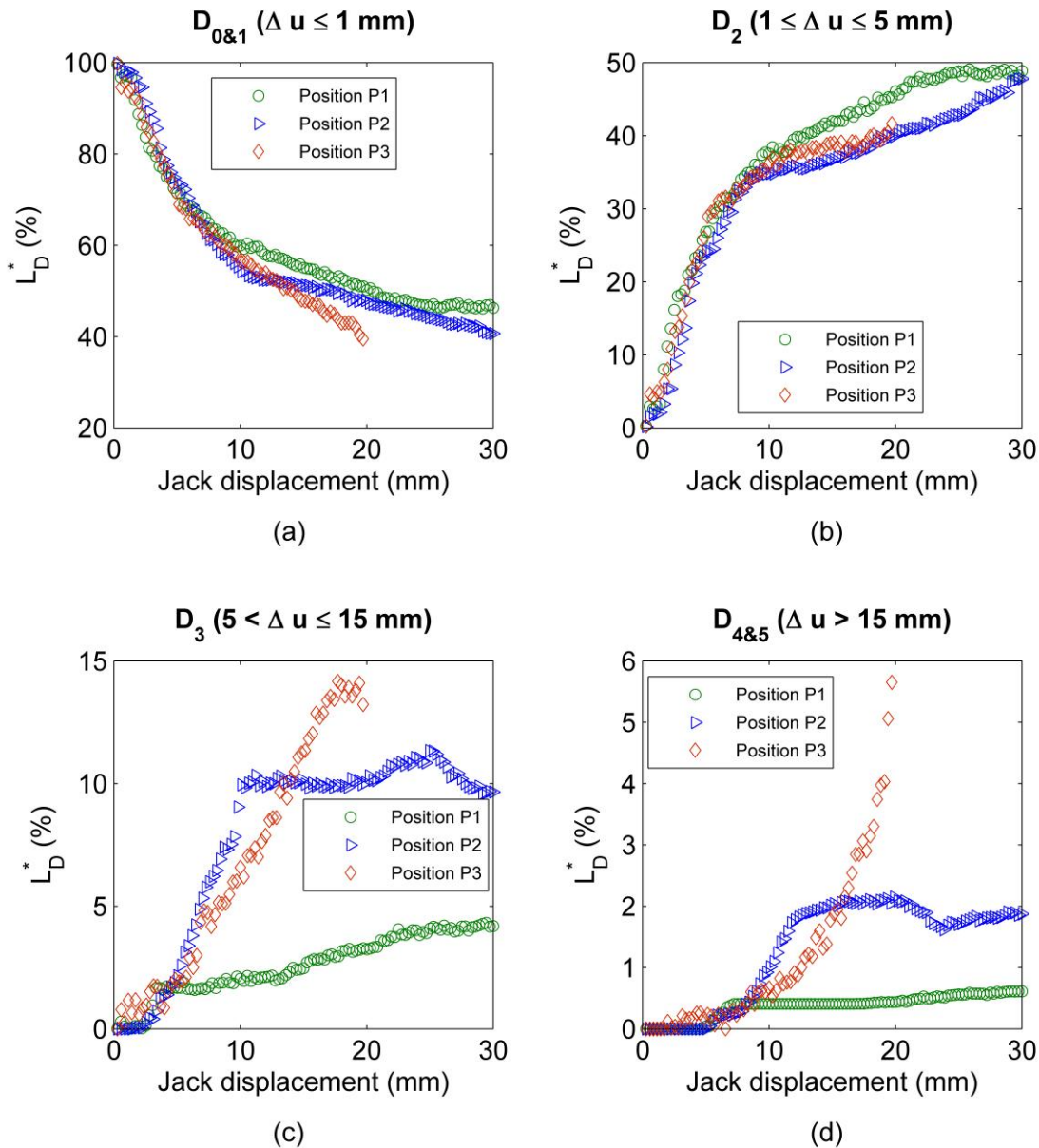


**Figure 6.** Total length of cracks associated with (a) classes  $D_{0\&1}$  ( $\Delta u \leq 1$  mm), (b) class  $D_2$  ( $1 \text{ mm} \leq \Delta u \leq 5$  mm), (c) class  $D_3$  ( $5 \text{ mm} < \Delta u \leq 15$  mm), and (d) classes  $D_{4\&5}$  ( $\Delta u > 15$  mm).  $L^*D$  is the relative length of the cracks.

The class  $D_{0\&1}$  corresponds to a crack width between 0 and 1 mm, which is affected by the measurement errors of DIC. Class  $D_2$  (1 to 5 mm) is linked to cracks that are slightly opened but do not play a significant role in a global behaviour of the structure. Incidentally, the three positions in Figures 6a-b show similar trends, which are the defaults of our physical model. As mentioned above, the model actually has some interfaces between blocks that are already opened, and the evolution of the subsidence trough can lead to a partial closure of these opened joints. To overcome this inconvenience, we can take both positive and negative values for  $\Delta u$  into account in Equation (3). Consequently, the first two classes are not analyzed in-depth.

Classes  $D_3$  and  $D_{4\&5}$  (Figures 6c-d), corresponding to the moderate and severe & very severe damage, show similar trends:  $P_1$  yields a linear curve;  $P_2$  presents a linear part when the vertical jack

displacement is smaller than 10 mm and a stationary part for the rest of the subsidence development; and  $P_3$  shows a mostly non-linear trend. In the final state, the values for the total length of the cracks exhibit significant differences:  $P_1$  represents 4.2%- $D_3$  and 0.6%- $D_{4\&5}$ ;  $P_2$  represents 9.6%- $D_3$  and 1.9%- $D_{4\&5}$ ; and  $P_3$  represents 13.2%- $D_3$  and 5.6%- $D_{4\&5}$ .  $P_3$  has the largest crack lengths, which leads to the most significant damage. This conclusion coincides well with the abovementioned conventional parameters.

Table 2 summarizes the damage evaluations for the different structures according to slope, deflexion, deformation, and total length of cracks.

**Table 2.** Comparison of the damage assessment parameters

| Displacement of jack | Position | Slope (according to [13]) | Deflexion (according to [3]) | Deformation (according to [1]) | Total length of cracks |
|----------------------|----------|---------------------------|------------------------------|--------------------------------|------------------------|
| 10 mm                | $P_1$    | Negligible damage         | Moderate damage              | Moderate damage                | Negligible damage      |
|                      | $P_2$    | High damage               | Severe to very severe damage | Severe to very severe damage   | Severe damage          |
|                      | $P_3$    | Moderate damage           | Severe to very severe damage | Severe to very severe damage   | Severe damage          |
| 20 mm                | $P_1$    | Moderate damage           | Severe to very severe damage | Moderate damage                | Moderate damage        |
|                      | $P_2$    | High damage               | Severe to very severe damage | Severe to very severe damage   | Severe damage          |
|                      | $P_3$    | High damage               | Severe to very severe damage | Severe to very severe damage   | Very severe damage     |
| 30 mm (final state)  | $P_1$    | Moderate damage           | Severe to very severe damage | Moderate damage                | Moderate damage        |
|                      | $P_2$    | High damage               | Severe to very severe damage | Severe to very severe damage   | Very severe damage     |
|                      | $P_3$    | Collapse                  | Collapse                     | Collapse                       | Collapse               |

## 5 CONCLUSION

In this study, a new point of view is proposed for crack identification in masonry with the use of physical modelling incorporating an experimental damage criterion. Three important properties of cracks have been indicated: location, width, and length for a damage-related performance evaluation. In particular, a damage indicator is developed in this paper that is associated with the total length of cracks. This indicator has numerous advantages compared to the conventional indicators, especially when evaluating local damage to the structure. Furthermore, the proposed indicator can be implemented in numerical models.

The investigation discussed the use of physical modelling to assess damage to masonry due to underground excavations. In our physical model, the elastic foundation is considered to be an element that transfers damage to the masonry wall. In fact, the deflexion of the foundation explains the location of cracks: numerous cracks appear in the maximal deflexion position. A series of tests has been conducted in order to study the damage for three critical positions, namely the sagging zone, hogging zone, and mixed zone. The results demonstrate that the mixed zone is the most dangerous, as evidenced by the numerous cracks on the surface of the structure and the total collapse at the end of the test. Meanwhile, the sagging zone has few cracks, and the structure should be classified as being in the moderate damage category. Finally, the structure in the hogging position also has numerous cracks, but no collapse is observed. This position should be in the severe & very severe damage class.

Research may be improved with more realistic models for masonry that take the windows, mortar, etc. into account.

## REFERENCES

- [1] Boscardin M, Cording E. Building Response to Excavation-Induced Settlement. *Journal of Geotechnical Engineering*. 1989;115:1-21.
- [2] Burland JB. Assessment of risk of damage to buildings due to tunnelling and excavation. *1st International Conference on Earthquake Geotechnical Engineering*. Tokyo, 1995.
- [3] Potts DM, Addenbrooke TI. A structure's influence on tunnelling-induced ground movements. *Proc Inst Civil Eng-Geotech Eng*. 1997;125:109-25.
- [4] Deck O, Singh A. Analytical model for the prediction of building deflections induced by ground movements. *International Journal for Numerical and Analytical Methods in Geomechanics*. 2012;36:62-84.
- [5] Giardina G, Marini A, Hendriks MAN, Rots JG, Rizzardini F, Giuriani E. Experimental analysis of a masonry façade subject to tunnelling-induced settlement. *Engineering Structures*. 2012;45:421-34.
- [6] Laefer DF, Hong LT, Erkal A, Long JH, Cording EJ. Manufacturing, assembly, and testing of scaled, historic masonry for one-gravity, pseudo-static, soil-structure experiments. *Construction and Building Materials*. 2011;25:4362-73.
- [7] Burland JB, Wroth CP. Settlement of buildings and associated damage. *Proceedings, Conference on Settlement of Structure*. Cambridge, Pentech Press, London., 1974.
- [8] Buckingham E. On Physically Similar Systems; Illustrations of the Use of Dimensional Equations. *Physical Review*. 1914;4:345-76.
- [9] Dehousse NM, Arnould R. Les modèles réduits de structures en génie civil. Dunod ed. Paris1971.
- [10] Al Heib M, Emeriault F, Caudron M, Nghiem L, Hor B. Large-scale soil-structure physical model (1g)-assessment of structure damages. *International Journal of Physical Modelling in Geotechnics*. 2013;13:138-52.
- [11] Deck O, Al Heib M, Homand F. Taking the soil–structure interaction into account in assessing the loading of a structure in a mining subsidence area. *Engineering Structures*. 2003;25:435-48.
- [12] VIC-3D. Testing guide 2010, projection error, bias and noise.: [www.correlatedsolution.com](http://www.correlatedsolution.com).
- [13] Loganatban N. An innovative method for assessing tunnelling-induced risks to adjacent structures. One Penn Plaza ed: Parsons Brinckerhoff Inc.; 2011.
- [14] Hor B. Evaluation et réduction des conséquences des mouvements de terrains sur le bâti: approches expérimentale et numérique. *Thesis, Institut National des Sciences Appliquées de Lyon*; 2012.